Electronic Supplementary Material (ESI) for Inorganic Chemistry Frontiers.

Supplementary material

A Compact Silicon-carbon Composite with Embedded Structure for High Cycling Coulombic Efficiency Anode Material in Lithium-ion Batteries

Wei Zhang, [a,b,c] Sheng Fang, [a,b] Ning Wang, [a,b] Jianhua Zhang, [a,b,c] Bimeng Shi, [a,b] Zhanglong Yu [a,b] and Juanyu Yang, *[a,b,c,d]

[a] *National Power Battery Innovation Centre, GRINM Group Co., Ltd., Beijing 100088, China*

[b] *China Automotive Battery Research Institute Co., Ltd., Beijing 100088, China*

[c] *General Research Institute for Nonferrous Metals, Beijing 100088, China*

[d] *National Engineering Research Center for Rare Earth Materials, GRINM Group Co., Ltd., Beijing 100088, China*

* Corresponding author: Juanyu Yang
E-mail: juanyuyang@163.com

Contents

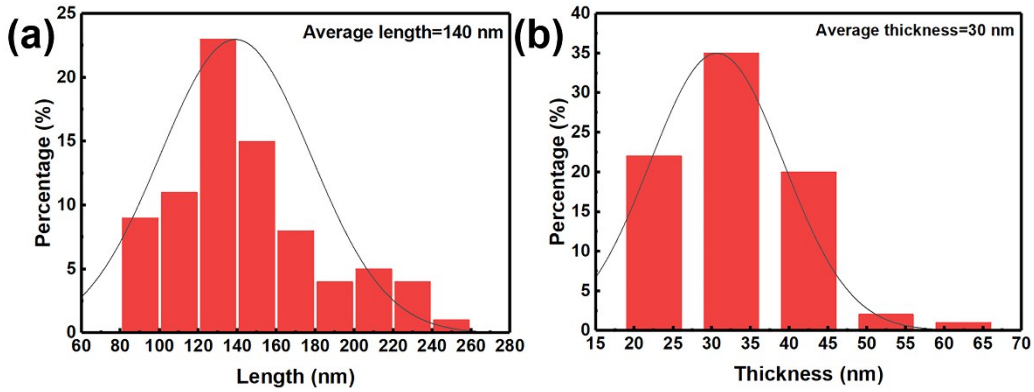

Fig. S1. The length (a) and thickness (b) size statistics of nano-silicon inside Si@C composite.

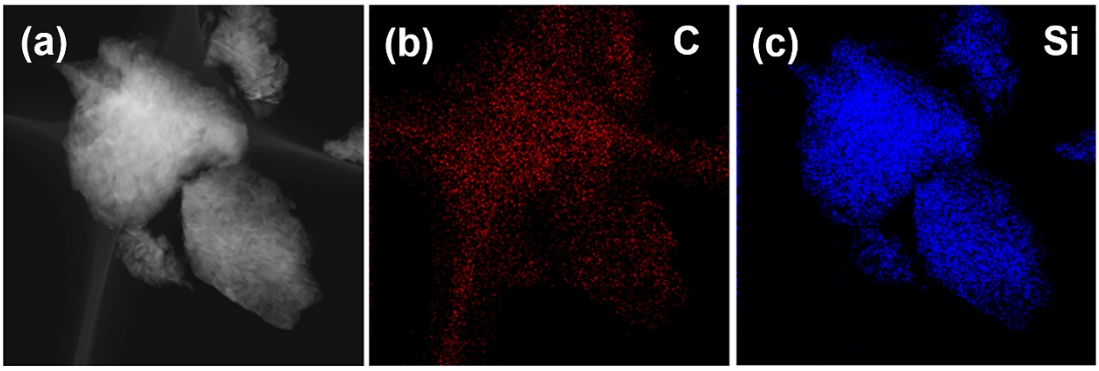

Fig. S2. TEM images (a) of Si@C composite and the corresponding elemental mapping of C (b) and Si (c).

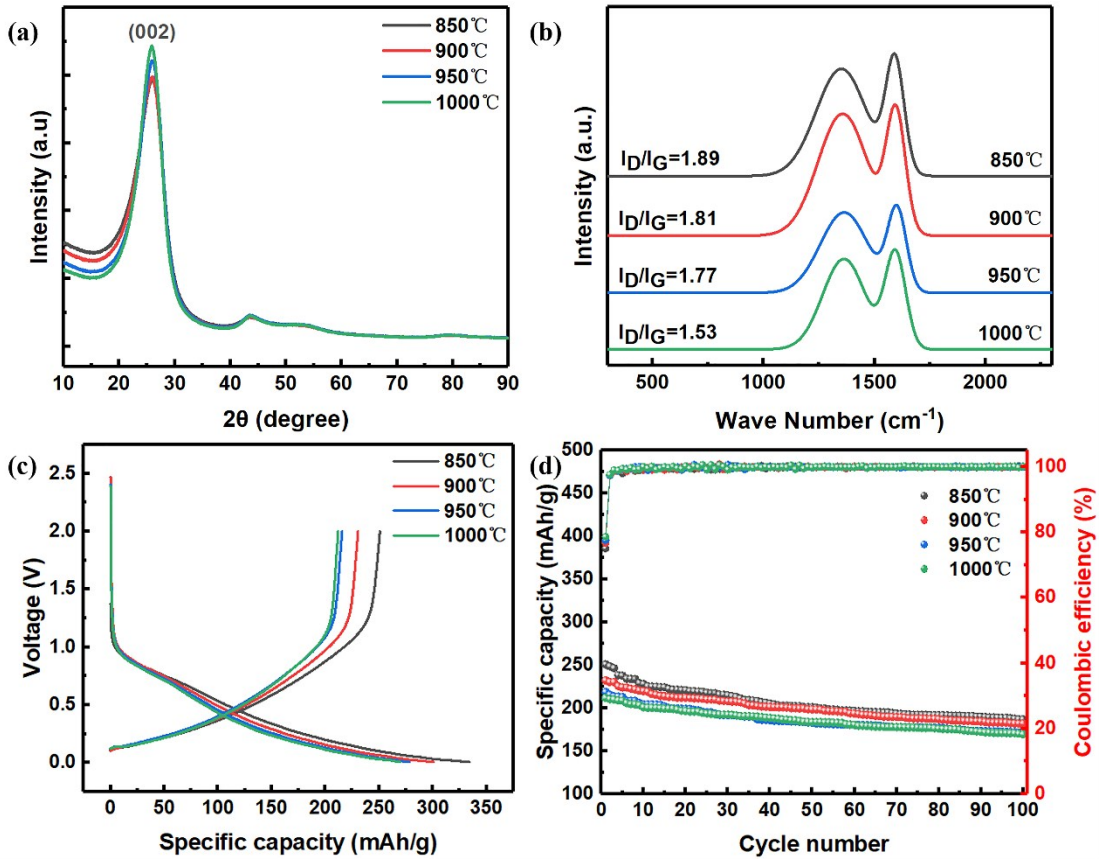

Fig. S3. XRD patterns (a), Raman spectra (b), the initial charge/discharge profile (c) and cycling performances (d) of the coal tar pitch pyrolytic carbon after the heat treatment at different temperature.

The structure and electrochemical properties of carbon are extremely important for silicon-carbon composite, especially silicon-carbon composite with high silicon content. We study the structure and electrochemical properties of coal tar pitch pyrolytic carbon (PC) heated treatment at different temperatures. As shown in Fig. S3a, we can find a broad peak in the range of 20-30° corresponding to the (002) lattice plane of the amorphous carbon from coal tar pitch. As the heat treatment temperature increases, the intensity of XRD diffraction peaks at the (002) lattice plane gradually increases, and the diffraction peaks become narrow, which indicate that the degree of graphitization of PC increases. To further verify the graphitization degree of PC, Fig. S3b shows the Raman spectra of PC at different temperature. The ratio of integrated area of the D band (disordered carbon) and G band (graphite carbon) at 1360 cm^{-1} and 1580 cm^{-1} reflect the graphitization degree. I_D/I_G decreases from 1.89 to 1.53 with increasing temperature, indicating that the graphitization degree of PC gradually increases, which corresponded to XRD results. Tab. S2 lists the electrochemical performance parameters of PC. According to the initial charge and discharge curve of PC in Fig. S3c, PC has the highest initial coulombic efficiency of 78.58% at 1000°C. After 100 cycles, the PC has a capacity retention of 80% at 1000°C.

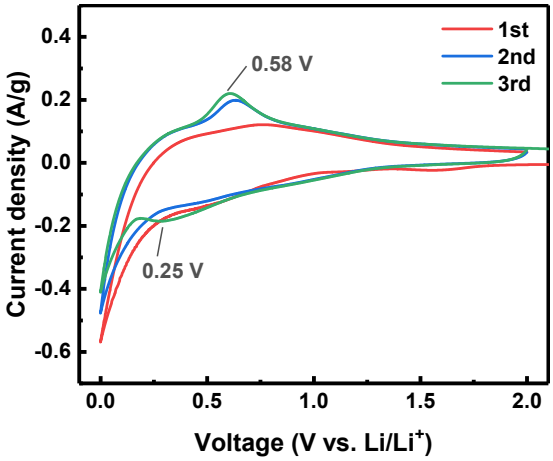

Fig. S4. The cyclic voltammetry (CV) curves of Si@C composite between 0.005 V and 2.000 V.

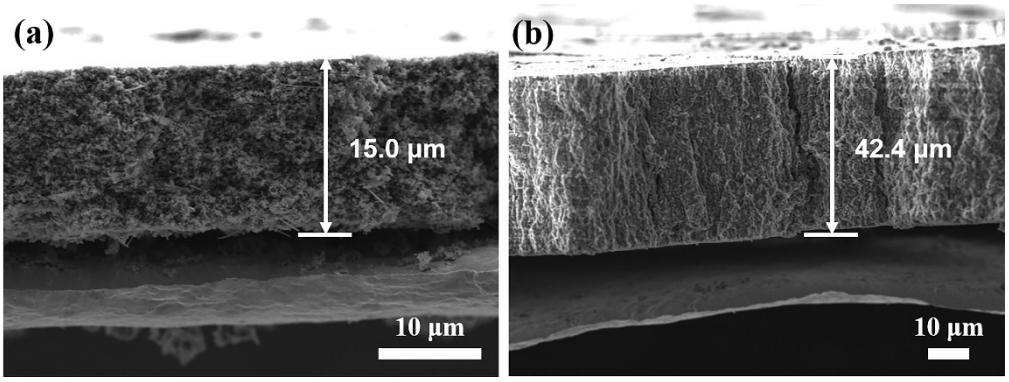

Fig. S5. The cross-sectional SEM images of nano-silicon electrodes at initial state (a) and after the 50th cycle (b).

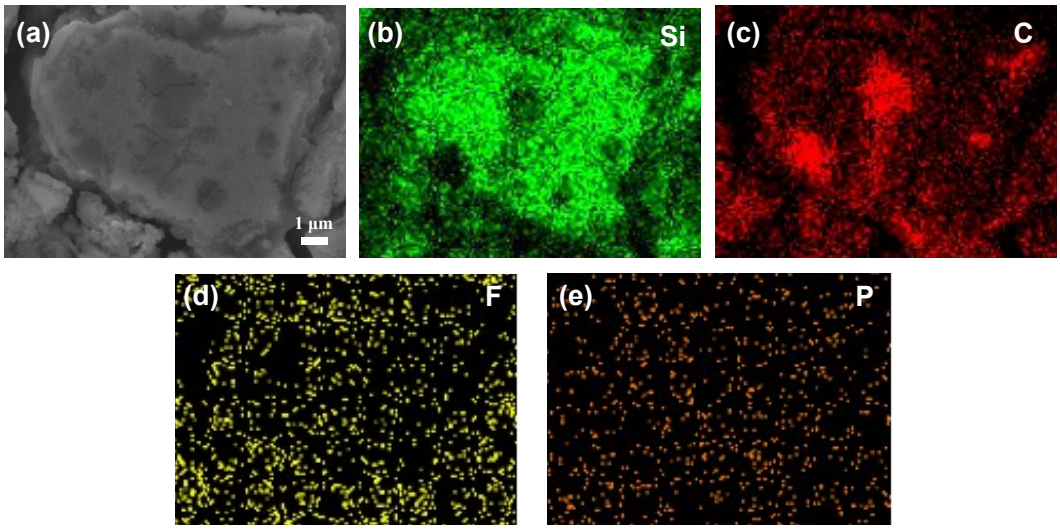

Fig. S6. The EDS elemental mapping of the cross-section of Si@C composite after the 50th cycle: (b) Si, (c) C, (d) F, (e) P.

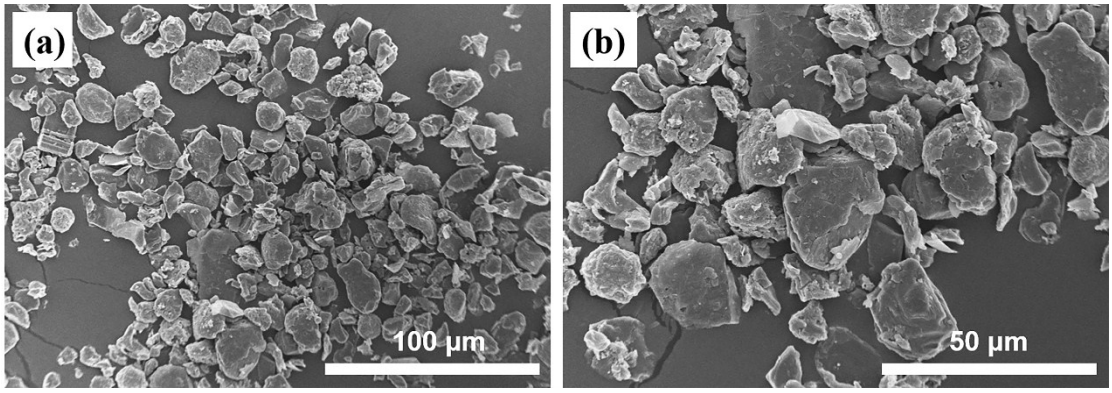

Fig. S7. The SEM images of 360G (a, b).

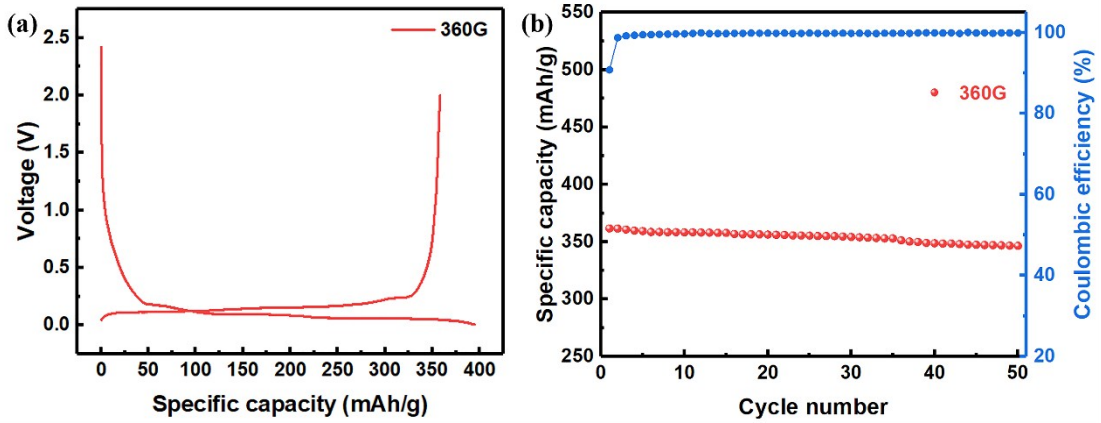

Fig. S8. The initial charge/discharge profile (a) and cycling performances (b) of 360G.

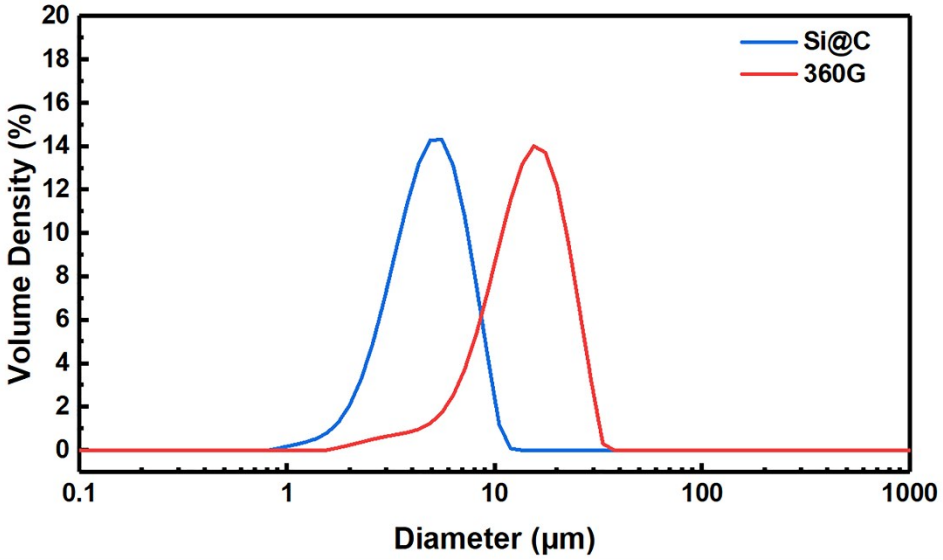

Fig. S9. The particle-size distributions of Si@C and 360G.

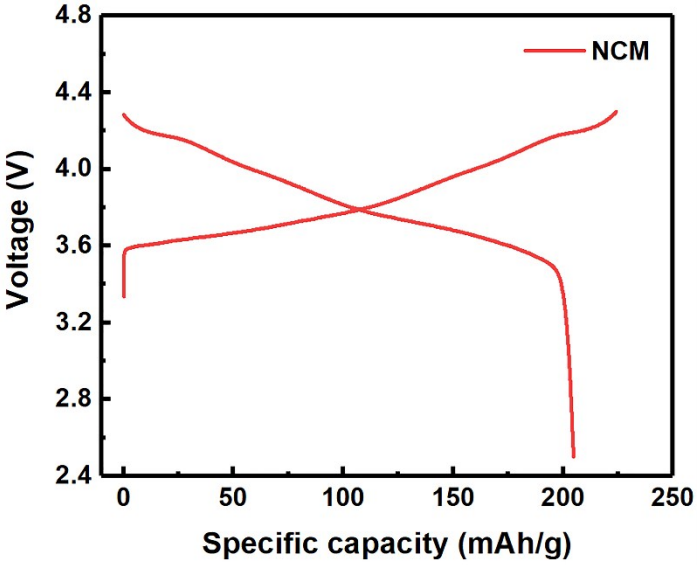

Fig. S10. The charge/discharge profile of NCM811.

Tab. S1. Laser particle size test results of nano-silicon dispersion.

	D_x10 (μm)	D_x50 (μm)	D_x90 (μm)
Nano-silicon	0.101	0.159	0.225

Tab. S2. The initial coulombic efficiency, specific capacity and capacity retention of PC at different temperatures.

Temperature (°C)	Initial CE (%)	Specific capacity (mA h g^{-1})	Capacity retention (%)
850	75.02	250.8	74.5
900	76.68	232.1	78.3
950	77.53	218.6	78.5
1000	78.58	211.7	80.0

Tab. S3. The impedance parameters for Si@C composite anodes after different cycles.

Cycle number	R_{SEI}/Ω	CPE1-T/F	CPE1-P	R_{ct}/Ω	CPE2-T/F	CPE2-P
20th	2.47	2.29E-5	0.58	19.64	6.40E-4	0.85
50th	5.65	3.14E-5	0.64	29.69	5.31E-4	0.87
100th	9.30	3.54E-5	0.63	40.32	2.15E-4	0.86

Tab. S4. The BET surface area and tap density of nano-silicon, 360G, Si@C and Si@C-G composite.

Materials	Tap density (g cm^{-3})	BET surface area (m^2 g^{-1})
Nano-silicon (agglomerates)	——	108.81
360G	0.89	2.64
Si@C	0.73	6.63
Si@C-G	1.0	3.92

Tab. S5. The average capacity and capacity retention of Si@C-G composite.

Rate (C)	Average capacity (mA h g^{-1})	Capacity retention (%)
0.1	662.02	100.00
0.2	656.88	99.22
0.5	654.36	98.84
1.0	650.82	98.31
2.0	645.32	97.47
0.1	658.44	99.46

Tab. S6. The electrochemical performance of various silicon-carbon composite

Ref. No.	Specific capacity/mA h g^{-1}	Initial CE/%	Average CE/%
1	517	92	<99.80 (10-50 cycles)
2	620	89.2	99.80 (10-500 cycles)
3	712	80.5	<99.50 (100 cycles)
4	640	90.5	99.80 (50-300 cycles)
Our work	669.5	83.76	99.88 (10-250 cycles)

References

1. M. Ko, S. Chae, J. Ma, N. Kim, H.-W. Lee, Y. Cui and J. Cho, Scalable synthesis of silicon-nanolayer-embedded graphite for high-energy lithium-ion batteries, Nature Energy, 2016, 1, 16113.
2. Q. Xu, J.-Y. Li, J.-K. Sun, Y.-X. Yin, L.-J. Wan and Y.-G. Guo, Watermelon-Inspired Si/C Microspheres with Hierarchical Buffer Structures for Densely Compacted Lithium-Ion Battery Anodes, Advanced Energy Materials, 2017, 7, 1601481.
3. S. Y. Kim, J. Lee, B.-H. Kim, Y.-J. Kim, K. S. Yang and M.-S. Park, Facile Synthesis of Carbon-Coated Silicon/Graphite Spherical Composites for High-Performance Lithium-Ion Batteries, Acs Applied Materials & Interfaces, 2016, 8, 12109-12117.

4 J. Y. Li, G. Li, J. Zhang, Y. X. Yin, F. S. Yue, Q. Xu and Y. G. Guo, Rational Design of Robust Si/C Microspheres for High-Tap-Density Anode Materials, ACS Applied Materials & Interfaces, 2019, 11, 4057-4064.